QUANTITATIVE ELECTRONIC STRUCTURE ANALYSIS OF α-AL_2O_3 USING SPATIALLY RESOLVED VALENCE ELECTRON ENERGY-LOSS SPECTRA

HARALD MÜLLEJANS*, J. BRULEY**, R. H. FRENCH*** AND P. A. MORRIS***
*Max-Planck-Institut für Metallforschung, Seestraße 92, D-70174 Stuttgart, Germany
**Lehigh University, Materials Science Department, Bethlehem, PA 18015-3195, USA
***DuPont Central Research and Development, Wilmington, DE 19880-0356, USA

ABSTRACT

Valence electron energy-loss (EEL) spectroscopy in a dedicated scanning transmission electron microscope (STEM) has been used to study the $\Sigma 11$ grain boundary in α-Al_2O_3 in comparison with bulk α-Al_2O_3. The interband transition strength was derived by Kramers-Kronig analysis and the electronic structure followed from quantitative critical point (CP) modelling. Thereby differences in the acquired spectra were related quantitatively to differences in the electronic structure at the grain boundary. The band gap at the boundary was slightly reduced and the ionicity increased. This work demonstrates for the first time that quantitative analysis of spatially resolved (SR) valence EEL spectra is possible. This represents a new avenue to electronic structure information from localized structures.

1. INTRODUCTION

The real and imaginary part of the dielectric function can be obtained from valence EEL spectroscopy by Kramers-Kronig analysis [1]. Such results have been compared qualitatively to optical data [2] but to date there has not been a quantitative evaluation of these measured optical properties or the electronic structure. By comparison quantitative CP analysis [3] [4] of vacuum ultraviolet (VUV) spectra has provided a detailed understanding of interband transitions and the electronic structure of ceramics such as α-Al_2O_3 [5] [6] and AlN [7]. VUV measurements are, however, limited to the determination of the bulk properties of a material, due to the large size of the optical probe. The importance of the electronic structure of localized features such as dislocations, twins and grain boundaries has motivated the combination of this quantitative analysis with SR spectroscopy.

Here we present our results from combining SR-EEL spectroscopy in a dedicated STEM, providing information on a nanometer scale, with quantitative analysis to investigate the electronic structure of α-Al_2O_3 in the bulk material and at the $\Sigma 11$ grain boundary. Although EEL spectroscopy in a dedicated STEM has been available for some time such studies were hindered by the lack of analytical tools for interpreting and comparing the electronic structure information content of the EEL data. Recent improvements in analytical techniques for VUV spectroscopy, namely CP analysis of the interband transition strength, have rendered such problems tractable. We believe that the present work is the first successful quantitative analysis of the electronic structure of a grain boundary. It leads the way to further work in this area, proving that analysis at nanometer dimensions is possible.

Mat. Res. Soc. Symp. Proc. Vol. 332. ©1994 Materials Research Society

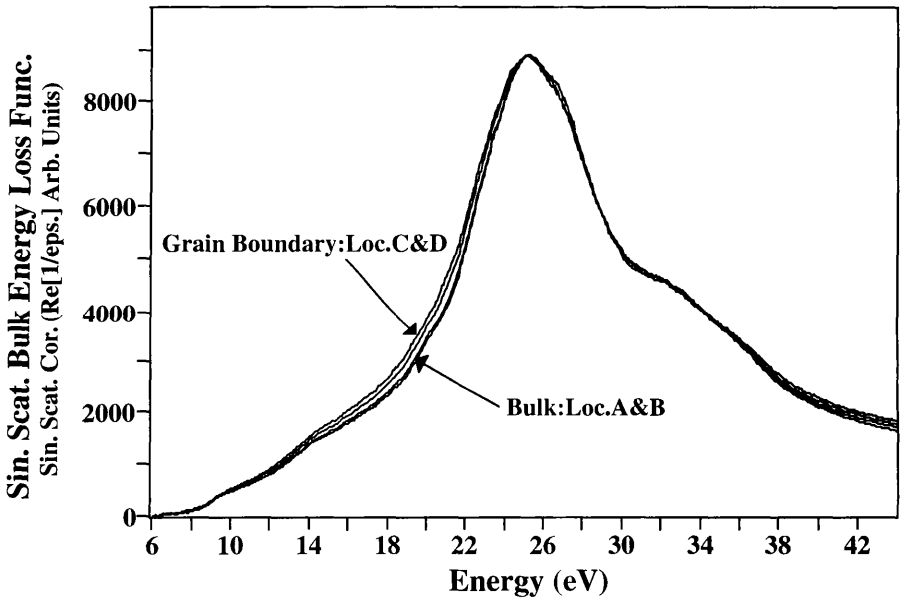

Figure 1. Single scattering corrected bulk energy-loss functions, acquired using STEM SR-EEL spectroscopy, taken at locations A and B in the bulk of each grain of the α-Al_2O_3 sample and at locations C and D along the Σ11 grain boundary.

2. EXPERIMENTS

A cross-section transmission electron microscopy sample of the near Σ 11 grain boundary in α-Al_2O_3 [8] was prepared by standard methods [9]. EEL spectra were acquired with a Gatan 666 parallel EEL spectroscopy system fitted to a Vacuum Generators HB501 dedicated STEM operating at 100 keV. The incident beam convergence and the collection semi-angle were both 7 mrad and the energy resolution was better than 0.7 eV. Spectra were acquired while the electron beam was scanning an area of 3 nm x 4.5 nm on the specimen, reducing beam damage and allowing for manual correction of specimen drift. Data analysis was done by the Gatan software El/P version 2.1, Kramers-Kronig analysis and CP modelling were performed by programs [10] [11] running under GRAMS/386 [12]. Four sets of spectra were taken, two with the electron beam on bulk α-Al_2O_3 on either side of the grain boundary (A and B) and two with the electron beam located on the Σ 11 grain boundary (C and D). To increase the dynamic range of the detector system each set contained three spectra (50 eV wide), with the following features just below saturation: the Al-L edge, the bulk plasmon and the zero loss. After correction of readout pattern and dark current of the detector the three spectra of each set were spliced together to give a single spectrum from -10 to 80 eV energy loss. The specimen was about 60 nm thick as determined by the ratio of inelastic to total spectrum intensity. The multiple scattering (MS) was removed by Fourier-log deconvolution [1]. There always remained a finite band-gap absorption intensity which may be caused in part by the zero-loss removal procedure employed by the Gatan routine, and in part due to energy losses resulting from relativistic retardation effects (Çerenkov and

transition radiation). A power law of the form $A*E^{-r}$, where A and r are constants and E the energy loss, was fitted in the band-gap region, extrapolated to 80 eV and subtracted from the data to remove the intensity arising from these effects. The resulting spectrum was corrected for the incident beam convergence and the finite collection angle at each energy loss with a program based on Egerton's CONCOR routine [1]. The four spectra resulting from this analysis are the single scattering distribution, two for bulk α-Al_2O_3 and two for the Σ 11 grain boundary (fig. 1). They show that changes in the energy-loss function of the bulk and boundary appear most prominently in the energy range from 14 to 26 eV on the low energy side of the bulk plasmon peak at 25 eV.

3. ANALYSIS

To enable quantitative analysis of the valence EEL spectra for interband electronic structure information it is important to understand any experimental and analytical artifacts which can arise in the data. The quantitative analysis presented here is based on an accurate knowledge of the amplitude of the single scattering EEL spectra so as to derive the interband transition strengths for CP analysis, permitting the accurate use of spectral strengths and amplitudes and for example the partial optical sum rules. Therefore here we consider the effects of the MS correction routines and the use of the index sum rule to scale the amplitude of the EEL spectra.

3.1 Multiple scattering analysis

The acquired EEL spectra must be corrected for MS events to derive the single scattering bulk energy-loss function. The routines used here for MS correction determine the scattering power by comparison of the zero loss peak to the rest of the EEL spectrum. By artificially multiplying the zero loss peak by factors of 0.5, 0.8. 0.9, 0.95, 1.0, 1.05, 1.1, 1.2 and 1.5 we can vary the imputed scattering power in the analysis. The results (fig. 2) demonstrate that the effect is appreciable only at energy losses beyond 34 eV. Upon Kramers-Kronig analysis of these EEL spectra, only for large MS errors changes are seen in the interband transition strengths (fig. 3) in the region from 8 to 26 eV where the band structure information appears in the data. Therefore the quantitative analysis is not very sensitive even to gross errors in the MS correction. Here have we used the accurate MS correction in all subsequent analysis.

3.2 Index Sum Rule

The complex optical property J_{CV} is defined by [7]

$$J_{CV}(E) = \frac{m^2}{8\,\pi^2\,h^2\,e^2}\,E^2\,\varepsilon(E) \qquad (1)$$

where m is the mass of the electron, h is Planck's constant and E is the energy loss. The complex dielectric function ε was calculated by Kramers-Kronig analysis with an FFT based algorithm [13] originally developed for VUV data and modified for EEL spectra. The real part of J_{CV} is called the interband transition strength. Since the EEL spectra are acquired as scattering counts versus energy, the data is in arbitrary units and during Kramers-Kronig analysis the index sum

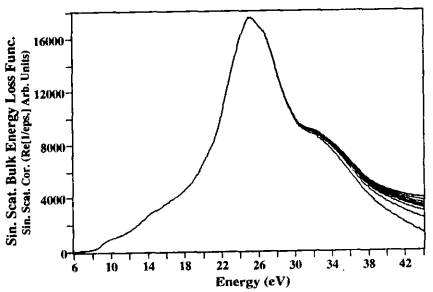

Figure 2. The effect of varying the multiple scattering correction on the single scattering distribution for the bulk α-Al_2O_3 SR-EEL spectrum taken at site A.

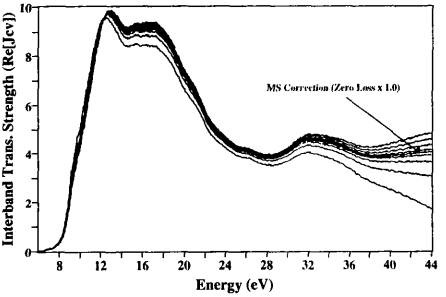

Figure 3. The effect of varying the multiple scattering correction on the interband transition strength J_{cv} determined from Kramers-Kronig analysis for the bulk α-Al_2O_3 SR-EEL spectrum taken at site A.

rule (Eq. 4.29 in [1]) is used to scale the y axis values of the EEL spectra. The J_{cv} spectra are very sensitive to varying the index of refraction from 1.5 to 2.2 (fig. 4). With large index errors the interband transition strength does change shape, emphasizing the importance of accurate knowledge of the index of refraction for analysis of EEL spectra. The index of refraction for α-Al_2O_3 used here is 1.767 at 633 nm (determined from optical spectroscopy), and is a constant for all spectra, so that consistent changes among the spectra are meaningful. For more complex systems where the index is unknown the use of the sum rule for scaling can be problematic and we are considering alternative methods for EEL spectra scaling.

After Kramers-Kronig analysis, a linear baseline was found to be present in the real part of the interband transition strength. The power law fit used to remove the intensity in the band gap region might cause such an offset at higher energies, since the extrapolation extends beyond the energies for which the effects of Çerenkov and transition radiation occur. This error might then propagate to yield the linear baseline in the real part of J_{cv} but at present the exact origin is still under investigation. For the following analysis in this work we have subtracted a linear baseline so that the intensity at 40 eV is reduced to zero. The interband transition strength then agrees closely with data determined from VUV spectroscopy [6]. Although this cannot be accepted as a full justification, it seems a reasonable way to proceed for the moment. Also it does not seem to be important for the comparison between bulk and grain boundary which is the main concern of this paper.

4. RESULTS

The interband transition strengths determined for bulk α-Al_2O_3 and the $\Sigma 11$ grain boundary are shown in fig. 5. The interband transitions in the bulk are identical while the two grain boundary results are different from the bulk and very similar to each other. The major difference seen in these spectra is a reduction of the interband transitions in the region of 14 to 22 eV. This demonstrates that the EEL spectra are accurate and reproducible and show the changes in the electronic structure between the bulk and the grain boundary. The interband transition strength for all four spectra was modeled with CPs for one exciton and three 3D bands in analogy to the analysis of VUV data [6]. The contributions from individual pairs of valence and conduction

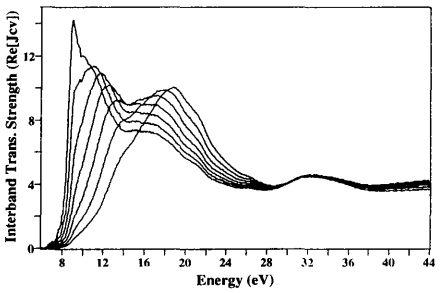

Figure 4. Effect of variation of the index of refraction in the sum rule used for scaling the EEL function on the resulting J_{CV} spectra.

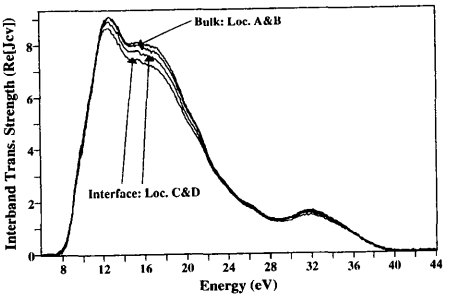

Figure 5. Comparison of the interband transition strengths of α-Al_2O_3 taken in the bulk at location A and B and at the Σ11 grain boundary at location C and D, showing the changes in the interband electronic structure at the boundary.

bands can be deduced from this analysis. In fig. 6 and 7 the individual CP models for the bulk and grain boundary are shown while these models are overlaid in fig. 8 and summarized in table I to highlight the changes in the interband transitions of the grain boundary. The EEL data agree with the interband transition strength obtained from VUV spectroscopy for bulk α-Al_2O_3 [6]. The exciton is a bound state of the excited electron and appears at ~ 9.1 eV. The three other sets of CPs used for modeling of the electronic structure correspond to transitions from the valence bands to the empty Al 3p band. The first set (lowest in energy) are transitions from the filled O 2p levels which represent the ionic bonding of the material. The next interband transition set arises from the hybridized Al=O level and can be thought of as the covalent part of the bonding in α-Al_2O_3. The third set are the interband transitions from the atomic like O 2s band.

Table I: Critical point parameters from STEM SR-EELS for bulk α-Al_2O_3 (location A and B, average) and the Σ11 grain boundary (location C and D, average).

		Energy (eV)		Amplitude		Width (eV)	
CP Set	**Type**	**Bulk**	**Σ11 GB**	**Bulk**	**Σ11 GB**	**Bulk**	**Σ11 GB**
Exciton		9.10	9.02	1.86	1.59	0.35	0.38
	M_0	9.20	9.13	1.14	1.13	0.07	0.07
O2p	M_1	11.64	11.50	0.43	0.43	0.07	0.08
	M_2	13.18	13.07	3.07	3.06	0.55	0.57
	M_3	22.53	22.58	1.49	1.52	0.86	0.94
	M_0	14.04	14.13	2.04	2.01	0.99	1.00
Al=O	M_1	16.50	17.72	0.19	0.16	0.35	0.56
	M_2	18.67	18.32	1.26	1.23	0.60	0.64
	M_3	27.87	28.20	0.63	0.65	0.85	0.85
	M_0	18.45	18.21	0.05	0.05	0.19	0.10
O2s	M_1	31.20	31.29	0.48	0.45	0.60	0.67
	M_2	32.83	33.30	0.27	0.34	0.79	0.83
	M_3	36.69	36.71	0.20	0.17	0.46	0.43

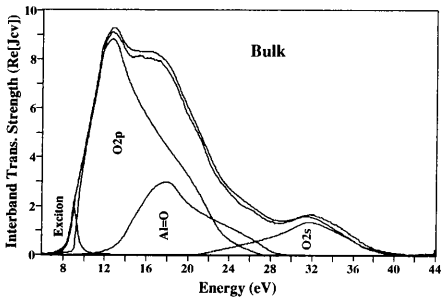

Figure 6. Interband CP models for bulk α-Al_2O_3 determined from STEM SR-EEL spectroscopy taken at location A and B.

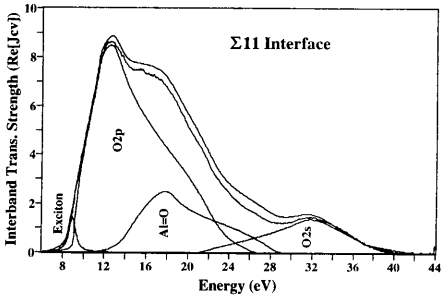

Figure 7. Interband CP models for the Σ11 grain boundary of α-Al_2O_3 from STEM SR-EEL spectroscopy determined at location C and D.

Partial optical sum rules (the oscillator strength sum rules) were calculated (table II) from the CP sets to determine the electron occupancy of the interband transitions in the bulk and at the boundary. These are calculated assuming a primitive unit cell volume of 84.9 angstroms^3 and 1 formula unit per unit cell. These results show that the electron occupancy of the Al=O hybridized bonding set is reduced in the boundary, and this can be seen by the changes in the % ionicity defined as Occ.(O2p)/{Occ.(O2p) + Occ.(Al=O)} which changes from 78.9 % ionic for the bulk to 80.8 % ionic at the Σ11 grain boundary.

5. DISCUSSION

The results for bulk α-Al_2O_3 and the Σ11 grain boundary show differences in the width of the band gap, the position of the exciton and in the strengths of the CP sets of interband transitions, most prominently in the A=O hybridized set. The latter is equivalent to an increase in ionicity at the grain boundary.

The decrease in the band gap width is less than 0.1 eV. In SR experiments investigating the energy-loss near-edge structure [14], it was found that the transition energy from the aluminium L shell to the conduction band was reduced by more than 1 eV. Hence the latter has to be attributed mainly to a shift in the core level energy. Such a combination of core and valence EEL spectroscopy gives full information about the electronic structure of materials. This could complement information obtained from various other spectroscopies, always with the added benefit of high spatial resolution.

Table II. Total and partial optical sum rules for bulk and Σ11 grain boundary of α-Al_2O_3, averaged for bulk and grain boundary locations

Electrons	Exper. Total	Model Total	Exciton	O2p	Al=O	O2s
Bulk	21.6	22.6	0.7	15.2	4.1	1.5
Σ11 GB	20.9	21.0	0.6	15.0	3.6	1.6

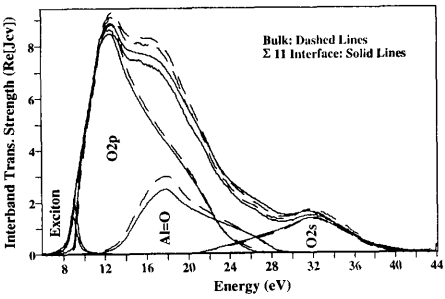

Figure 8 Interband CP models for the bulk (dashed) and Σ11 grain boundary (solid) of α-Al_2O_3 from STEM SR-EEL spectroscopy determined at location A and C, showing changes in exciton and the Al=O hybridized bonding CP set.

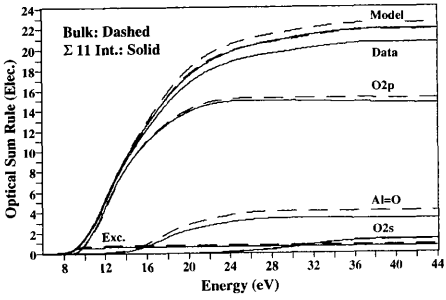

Figure 9. Total and partial optical sum rules showing the electron occupancies of the data, the model and each individual CP set for the bulk and Σ11 grain boundary in α-Al_2O_3.

In order to deduce relevant information about the electronic structure extensive data analysis has to be performed. It is important to ensure that the results of each step are reliable and reproducible as artefacts introduced in one step might give unreliable results concerning the electronic structure. The data analysis is analogous to the, now well established, analysis of VUV data once the dielectric function has been obtained. In the EEL specific part of the analysis the errors in the MS correction, while changing the interband transition strength, do not have a major influence on the final result. The index of refraction on the other hand has to be known accurately, which will be a problem for materials where no other information is available a priori. At two points in the analysis an intensity occurred which was subtracted ad hoc: in the band gap region of the single scattering distribution by a power law fit and in the real part of the interband transition strength by a linear baseline. The second effect might actually be caused by the first. Although the modifications used in the analysis cannot be fully justified, it seems to be reasonable to apply them because the data are then very similar to the results of VUV spectroscopy on bulk α-Al_2O_3.

The determination of the electronic structure without any prior information will only be reliable if the data analysis can made fully comprehensive. To achieve this the study of bulk α-Al_2O_3 is an ideal test case as its electronic structure is well known from VUV experiments. Nevertheless it is already possible now to deduce information about the relative electronic structure of localized features, i. e. in comparison to the bulk properties. All the influences of data analysis are expected to be similar, if not identical, for such spectra, which are similar to each other. Hence it is possible to deduce differences in electronic structure from differences seen in the EEL spectra taken at different locations on the specimen.

If we consider that the atomic structure at the Σ11 grain boundary is only changed in a region 0.6 - 0.8 nm wide at the grain boundary, as deduced from high resolution transmission electron microscopy [15], atomistic modelling [16] and the energy-loss near-edge structure [14], then only 20 - 25 % of the atoms in the probed volume contribute to the difference in electronic structure at the boundary. This means that the changes in electronic structure at the boundary are 4 - 5 times stronger than is seen directly from the data. Since the experiment is obviously sensitive to such small variations, it should be straightforward to investigate other, more extended inhomogeneities.

An important question concerns the reliability of the measurements (fig. 1) and the resulting differences (fig. 5). EEL measurements were reproducible, including the small shift in band gap energy. The system is stable to much less than 0.1 eV and an internal absolute energy reference is provided in each spectrum through the zero loss. Variations in spectra from the grain boundary represent variations in grain boundary structure. CP modelling is well established and numerically

stable. For the comparison of two spectra the present stability of data analysis is sufficient, whereas improvement is needed for fully quantitative results from a single spectrum. Noise is negligible compared to systematic errors. The work presented is a successful first attempt to investigate the electronic structure of a model grain boundary, demonstrating feasibility and suggesting ways for improvement. The boundary chosen is well characterized by HREM and atomistic structure modelling and work is in progress to calculate the electronic structure for a comparison with the present experimental results.

6. CONCLUSION

We have shown that it is possible to analyze SR-EEL spectra taken from bulk material and a grain boundary quantitatively. Differences in the raw experimental data have been translated into differences in the electronic structure. While the data analysis is not fully developed yet, we are confident that, in the application presented here and similar cases, the combination of SR-EEL spectroscopy and quantitative analysis yields valuable insight into the local electronic properties of materials. This opens up the quantitative analysis on a nanometer scale, for example of dislocations, defects, interfaces and intergranular glass films or materials which only exist as thin films or small particles. The knowledge of the electronic structure of small features is the key to our understanding of the mechanical and electrical properties of materials or devices incorporating them.

ACKNOWLEDGEMENTS

We acknowledge financial support from the Volkswagen-Stiftung contract I/ 66 790 for the Gatan PEELS and one of us (HM). We thank M. Rühle, P. Kenway and T. Höche for helpful discussions and S. Loughin, D. J. Jones and L. K. Denoyer for assistance.

REFERENCES

1. R. F. Egerton, Electron energy-loss spectroscopy in the electron microscope, (Plenum Press, New York, 1986).
2. M. G. Walls, PhD thesis, University of Cambridge, 1987.
3. S. Loughin, R. H. French, W. Y. Ching, Y. N. Xu and G. A. Slack, Appl. Phys. Lett. **63**, 1182 (1993).
4. S. Loughin, L. DeNoyer and R. H. French, Phys. Rev. B **to be submitted,** (1993).
5. R. H. French, J. Am. Ceram. Soc. **73**, 477 (1990).
6. R. H. French, D. J. Jones and S. Loughin, J. Am. Ceram. Soc. **submitted to Topical Issue on the Science of Alumina,** (1994).
7. S. Loughin, PhD thesis, University of Pennsylvenia, 1992.
8. P. A. Morris, PhD thesis, MIT, 1986.
9. B. D. Flinn, M. Rühle and A. G. Evans, Acta metall. **37**, 3001 (1989).
10. Critpt, v. 7.7, Spectrum Square Associates, Ithaca NY 14850 USA.
11. KKgrams, v. 3.4, Spectrum Square Associates, Ithaca NY 14850 USA.
12. Grams/386, v. 2.03, Galactic Industries, Salem NH.
13. M. L. Bortz and R. H. French, Appl. Spectr. **43**, 1498 (1989).
14. J. Bruley, Microsc. Microanal. Microstruct. **4**, 23 (1993).
15. T. Höche, P. R. Kenway, H.-J. Kleebe, M. Rühle and P. A. Morris, J. Am. Ceram. Soc. **submitted to Topical Issue on the Science of Alumina,** (1994).
16. P. R. Kenway, J. Am. Ceram. Soc. **submitted to Topical Issue on the Science of Alumina,** (1994).